ARTICLES
PUBLISHED ONLINE: 14 OCTOBER 2012 | DOI: 10.1038/NPHYS2441
nature physics

Strong Coulomb drag and broken symmetry in double-layer graphene

R. V. Gorbachev[1], A. K. Geim[1,2]*, M. I. Katsnelson[3], K. S. Novoselov[2], T. Tudorovskiy[3], I. V. Grigorieva[1,2], A. H. MacDonald[4], S. V. Morozov[2,5], K. Watanabe[6], T. Taniguchi[6] and L. A. Ponomarenko[1,2]*

Coulomb drag is a frictional coupling between electric currents flowing in spatially separated conducting layers. It is caused by interlayer electron–electron interactions. Previously, only the regime of weak ($d \gg l$) to intermediate ($d \sim l$) coupling could be studied experimentally, where d is the interlayer separation and l is the characteristic distance between charge carriers. Here we use graphene–boron-nitride heterostructures with d down to 1 nm to probe Coulomb drag in the limit $d \ll l$ such that the two Dirac liquids effectively nest within the same plane, but can still be tuned and measured independently. The strongly interacting regime reveals many unexpected features. In particular, although drag vanishes because of electron–hole symmetry when either layer is neutral, we often find drag strongest when both layers are neutral. Under this circumstance, drag is positive in zero magnetic field but changes its sign and rapidly grows in strength with field. The drag remains strong at room temperature. The broken electron–hole symmetry is attributed to mutual polarization of closely spaced interacting layers.

Since the first observation of Coulomb drag in GaAlAs heterostructures[1–3], double-layer electronic systems have been attracting unwavering interest (for review, see refs 4,5). A number of new interaction phenomena have been reported, which appear owing to many-body ground states formed jointly by charge carriers from both layers. These phenomena include even-denominator fractional quantum Hall states[6–8] and interlayer excitonic superfluidity[4,9–13]. It is believed that stronger interactions could lead to excitonic superfluidity at higher temperatures (T) and open new avenues for fundamental research and applications[14,15].

Until recently[16], GaAlAs heterostructures with two quantum wells separated by a relatively thin tunnel barrier (effective d down to 15 nm) were the only experimental systems allowing reliable measurements of Coulomb drag[1–13,17]. The advent of graphene–boron-nitride heterostructures[18,19] offers a double-layer system with much stronger interlayer interactions. First, charge carriers in graphene are confined within a single atomic plane and a few atomic layers of hexagonal boron nitride (hBN) are sufficient to isolate graphene electrically[19–21]. This allows double-layer heterostructures with $d \sim 1$ nm, an order of magnitude smaller than achieved previously. Second, the relatively small dielectric constant of hBN ($\varepsilon \approx 4$) also helps to increase the interaction strength. Third, charge carriers in graphene can be continuously tuned between electrons (e) and holes (h) from densities $n > 10^{12}$ cm^{-2} all the way to the neutral state where $l = 1/n^{1/2}$ nominally diverges. This makes it possible to access the limit $d/l \ll 1$ or, effectively, zero layer separation. Fourth, Coulomb drag in graphene heterostructures can be studied not only in the conventional Fermi liquid regime (where the Fermi energy E_F is larger than k_BT) but also in the little explored Boltzmann regime ($E_F < k_BT$). These features suggest a unique venue for searching for new interaction phenomena. Accordingly, double-layer graphene has attracted significant theoretical interest and has already become a subject of intense debates about predictions for both Coulomb drag[22–28] and excitonic superfluidity[15,29]. As for experiment, a recent publication[16] reported Coulomb drag in double-layer graphene in zero magnetic field B by using devices in which the layers were separated by a several-nanometre-thick alumina barrier and had charge carrier mobilities $\mu \sim 10{,}000$ cm^2 V^{-1} s^{-1}.

Here, we describe strong Coulomb drag and its anomalous behaviour in graphene–hBN heterostructures with mobilities $\mu \sim 100{,}000$ cm^2 Vs^{-1} and d down to 1 nm (trilayer hBN). In zero B and away from the neutrality point, we find the standard quadratic T dependence of the drag resistivity ρ_{drag}, a hallmark of Coulomb drag between degenerate Fermi liquids. By varying n and T, we observe a crossover between the Fermi liquid ($E_F \gg k_BT$) and interacting Boltzmann gas ($E_F < k_BT$) regimes, which shows up as a clear maximum in drag at $E_F \approx 2k_BT$. In the former regime, the dependences on n and d are much weaker than those found in GaAlAs heterostructures, and drag changes little for $d < 4$ nm, indicating that the limit of zero d is reached. These results generally agree with the theory developed recently for $d < l$ (refs 26,27). However, we find significant differences too. Most of them appear in the regime where both graphene layers are neutral and drag should be zero for symmetry considerations. Unexpectedly, the neutral state exhibits non-zero and, often, strongest drag. It is positive in zero B but changes the sign and rapidly grows in relatively weak $B = 0.1$–$1T$. We explain the positive drag in terms of interaction-induced correlations between e and h puddles in the two layers. The strong negative magneto-drag is attributed to interlayer exciton-like correlations between half-filled zero Landau levels.

[1]Centre for Mesoscience and Nanotechnology, University of Manchester, Manchester M13 9PL, UK, [2]School of Physics and Astronomy, University of Manchester, Manchester M13 9PL, UK, [3]Institute for Molecules and Materials, Radboud University of Nijmegen, 6525 AJ Nijmegen, The Netherlands, [4]Department of Physics, University of Texas at Austin, Austin, Texas 78712, USA, [5]Institute for Microelectronics Technology, 142432 Chernogolovka, Russia, [6]National Institute for Materials Science, 1-1 Namiki, Tsukuba, 305-0044, Japan. *e-mail: leonid.ponomarenko@manchester.ac.uk; geim@man.ac.uk.

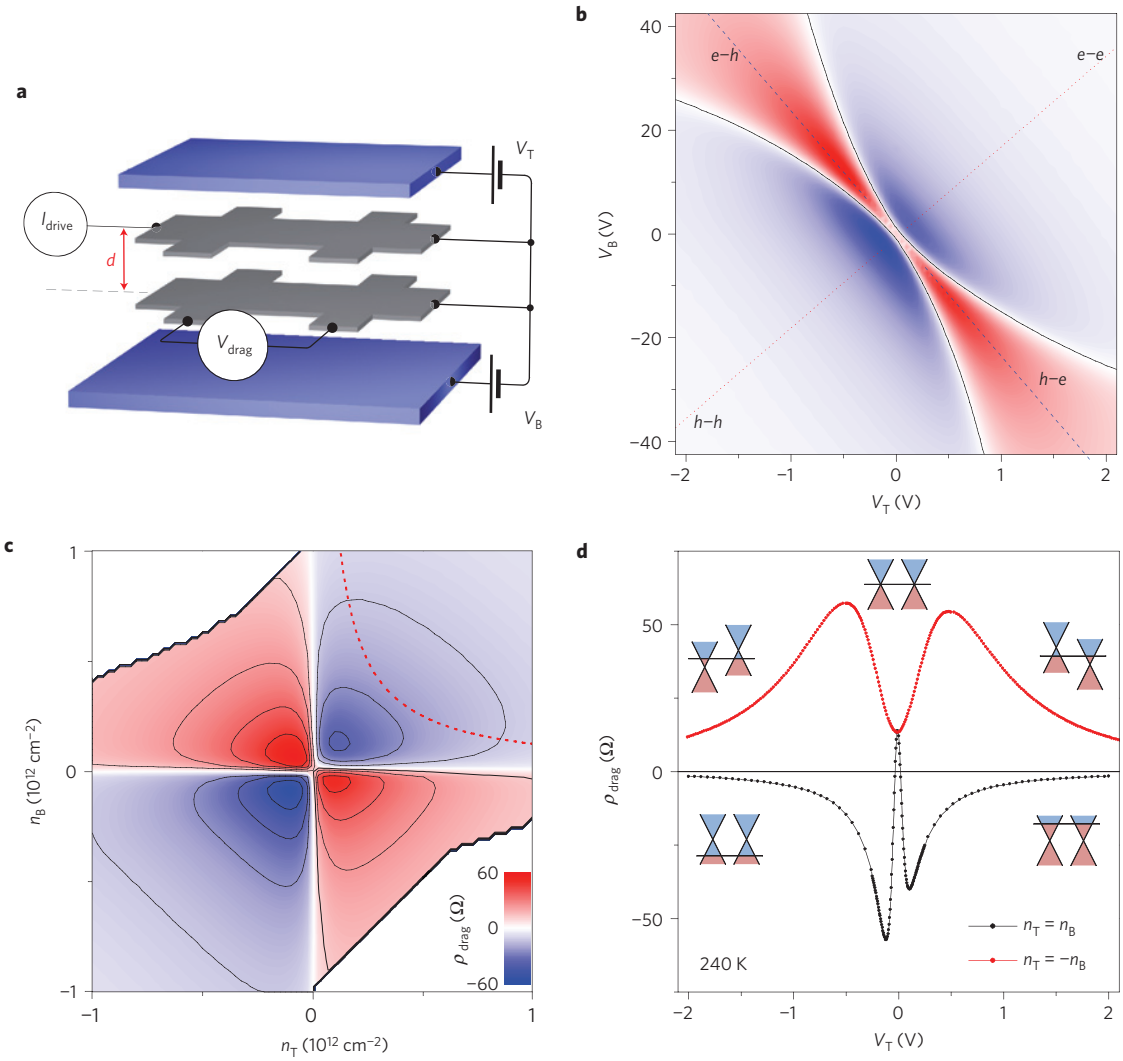

Figure 1 | Coulomb drag in double-layer graphene heterostructures in zero magnetic field. a, Schematic of our devices and measurements. **b**, ρ_{drag} as a function of V_T and V_B for a device with a trilayer hBN spacer ($d \approx 1$ nm). The black curves indicate zero-lines of ρ_{drag}; the colour scale is ± 60 Ω (see the inset in **c**). $T = 240$ K: in most cases, this was our highest T, chosen to be sufficiently close to room temperature and, at the same time, to prevent device damage that often occurred above 240 K. The device exhibits little chemical doping ($\ll 10^{11}$ cm^{-2}) and, for clarity, V_T and V_B are offset to zero at the dual neutrality point. **c**, ρ_{drag} from **b** replotted as a function of n_T and n_B. The solid curves are isolevels at every 12 Ω. The blank regions separated by thick lines contain no data. The dashed curve illustrates the functional dependence expected in the weakly interacting regime, $\rho_{drag} = f(n_T \times n_B)$. **d**, Behaviour of ρ_{drag} under the equal density conditions, $n_T = -n_B$ and $n_T = n_B$, which are indicated in **b** by the dashed and dotted lines, respectively. ρ_{drag} in **d** is plotted as a function of V_T; V_B is varied so that the densities are kept equal, allowing a common x axis for **b** and **d**. The Dirac-cone diagrams illustrate various doping regimes.

Devices and measurements

The schematics of our experiments are shown in Fig. 1a. The devices consist of two graphene monolayers separated by a thin hBN spacer. This double-layer structure is encapsulated between relatively thick (>20 nm) hBN crystals. The encapsulation is important to achieve high μ and little charge inhomogeneity δn (refs 18,19,30). The entire heterostructure is assembled on top of an oxidized Si wafer that serves as a bottom electrode. Carrier densities n_T and n_B in the top and bottom layers, respectively, are controlled by voltages V_T and V_B applied to the top and bottom electrodes. The two graphene layers are shaped into multi-terminal Hall bars (width of 1–2 μm), which are aligned on top of each other. By measuring longitudinal and Hall resistivities (ρ and ρ_{xy}, respectively) we can fully characterize each layer[18,19]. In particular, the positions of the neutrality point as a function of V_T and V_B are identified by zeros in ρ_{xy} (peaks in ρ_{xx}). Away from the neutrality point, $\rho_{xy} = B/ne$ and the Hall measurements yield n (e is the electron charge). This allows us to find n_T and n_B as a function of V_T and V_B. Details about our devices' fabrication and characterization can be found in the Supplementary Information and in refs 18,19,30.

Drag measurements were carried out by applying current I_{drive} through one graphene layer, and measuring the induced voltage V_{drag} in the second layer. The observed linear response $V_{drag} \propto I_{drive}$ allows us to present experimental data in terms of ρ_{drag} that is found to scale in the conventional manner with the width and length of the Hall bars. Typically, the top layer has a lower quality ($\mu_T \approx 30{,}000$ to 90,000 cm^2 V^{-1}s^{-1}) and we employ it as the drive layer. Higher-quality bottom graphene ($\mu_B \approx 50{,}000$–$120{,}000$ cm^2 V^{-1}s^{-1}) is used as the drag layer. If the drive and drag layers are interchanged, ρ_{drag} does not change, that is, the Onsager relation holds.

For hBN spacers down to 3 atomic layers in thickness, the tunnelling resistance is sufficiently high (>1 MΩ at low bias) and independent of T (refs 19–21) to ensure a negligible contribution of interlayer tunnelling to the measured voltage signal

(Supplementary Information). The interlayer resistance becomes unacceptably low for bilayer hBN ($\sim 10\,\mathrm{k}\Omega$). This implies that $d = 1\,\mathrm{nm}$ is the minimum separation that can realistically be achieved in drag experiments. In some measurements, we have applied interlayer voltage V_{int} that conveniently results in equal doping $n_{\mathrm{T}} = -n_{\mathrm{B}}$ (positive and negative n are assigned to e and h, respectively). However, the last approach is impractical for $d < 4\,\mathrm{nm}$ because the tunnel current increases with bias, effectively limiting the electrical doping achievable by V_{int} to $<10^{11}\,\mathrm{cm}^{-2}$ for small d.

Coulomb drag in zero magnetic field

Figure 1b shows ρ_{drag} as a function of V_{T} and V_{B} for one of our thinnest devices. There are 4 distinct segments, which correspond to different combinations of electrons and holes in the two layers. If both layers contain carriers of the same (opposite) sign, ρ_{drag} is negative (positive)[1–13,22–28]. The absolute value of ρ_{drag} exhibits a maximum in each of the 4 segments at low carrier densities. The condition of zero drag is shown by the solid curves, which (closely but not exactly) follow the neutrality points. The pronounced asymmetry between the size of the red and blue segments is due to a large quantum capacitance contribution for small d, which results in strongly nonlinear functions $n_{\mathrm{T,B}}(V_{\mathrm{T,B}})$ (refs 16,18,31,32). These were determined experimentally and modelled theoretically, which allows us to replot the data from Fig. 1b as a function of n_{T} and n_{B}. In the last representation (Fig. 1c), we recover nearly perfect 4 quadrant symmetry.

To get a closer look at the behaviour of Coulomb drag, we reduce the available parameter space to the symmetric situation in which e and h densities in both layers are equal. This matching density regime has been attracting particular attention[3–15]. The conditions $n_{\mathrm{T}} = \pm n_{\mathrm{B}}$ are marked in Fig. 1b by the dashed and dotted lines. Figure 1d shows changes in ρ_{drag} along these lines. One can see that, for e–h drag, ρ_{drag} exhibits a relatively simple, double-humped behaviour, which is easy to understand: drag has to decrease with increasing n as well as to disappear in neutral graphene. This necessitates maxima in ρ_{drag} at a finite $|n|$. In the case of e–e and h–h drag, ρ_{drag} has the opposite sign but exhibits roughly the same double-humped shape, except for a quicker response to V_{T} (see Fig. 1b,c). The main difference between the two curves in Fig. 1d appears near the dual neutrality point where $\rho_{\mathrm{drag}}(n_{\mathrm{T}} = n_{\mathrm{B}})$ changes its sign to reach the same positive value as $\rho_{\mathrm{drag}}(n_{\mathrm{T}} = -n_{\mathrm{B}})$. The region of positive drag at the dual neutrality point is also seen as a narrow gap between the curves marking zero ρ_{drag} in Fig. 1b. Positive drag at the dual neutrality point has been observed at $T > 50\,\mathrm{K}$ and zero B for all our devices. This observation implies broken e–h symmetry.

Strongly interacting Dirac liquids: comparison with theory

We first examine drag's behaviour away from the neutrality point, in the Fermi liquid regime studied extensively by theory. We focus below on the case of equal e–h densities ($n_{\mathrm{T}} = -n_{\mathrm{B}} \equiv n$), chosen for both simplicity and the theoretical interest it attracts. By measuring curves such as shown in Fig. 1d at different T, we have found that $\rho_{\mathrm{drag}} \propto T^2$ for sufficiently high n ($E_{\mathrm{F}} > 3k_{\mathrm{B}}T$). Examples of this behaviour are shown in Fig. 2a and in the Supplementary Information. The T^2 dependence is expected for any interaction strength d/l between graphene layers[22–28], provided that the carriers form a Fermi liquid state.

As for the d dependence, we find that ρ_{drag} varies approximately as $1/d^2$ (Fig. 2b) for large $d > 4\,\mathrm{nm}$; that is, much slower than $1/d^4$ expected in the weakly interacting regime. Moreover, our devices show practically no increase in drag below 4 nm, in qualitative agreement with theory[26,27] that predicts $\rho_{\mathrm{drag}}(d)$ to saturate at small d (Fig. 2b). Another significant difference with respect to weakly interacting systems is the observed functional dependence. In the $d > l$ case, theory expects ρ_{drag} to be a function f of the product $n_{\mathrm{B}} \times n_{\mathrm{T}}$ (refs 22–28), which should have resulted in strongly curved isolevels such as shown by the dashed curve in Fig. 1c. Instead, we observe flat isolevels, which imply that ρ_{drag} is closely described by the functional dependence $f(n_{\mathrm{B}} + n_{\mathrm{T}})$ (note that some other f can also yield nearly flat isolevels). This behaviour is robust and exemplified further in the Supplementary Information. The

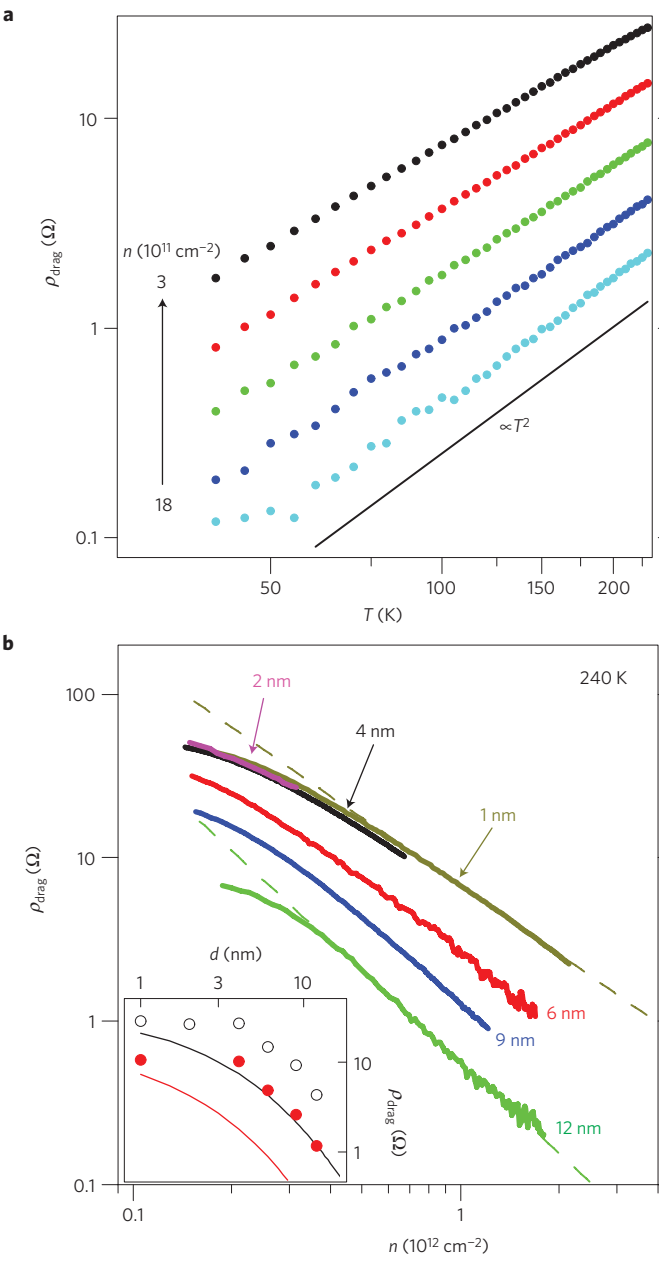

Figure 2 | Functional dependences of Coulomb drag away from the neutrality point. a, ρ_{drag} as a function of T for various n between 3 and 18 $\times 10^{11}\,\mathrm{cm}^{-2}$; $d \approx 6\,\mathrm{nm}$; $B = 0$. The solid line shows the expected functional dependence. Our devices are several micrometres in size and, at low T, exhibit strong mesoscopic (interference) fluctuations, which are observed in both drag and resistivity. This limits the T range in which quantitative comparison with the theory is possible to $T > 40\,\mathrm{K}$. To investigate Coulomb drag at lower T would require much larger devices. **b**, ρ_{drag} as a function of n and d. The dashed lines are fits to $1/n^{\alpha}$ with $\alpha \approx 1.3$ and 1.8 for $d = 1$ and 12 nm, respectively. The inset shows ρ_{drag} as a function of d for $n = 3$ and $7 \times 10^{11}\,\mathrm{cm}^{-2}$ (open and filled symbols, respectively). The solid curves are theory plots for these two n in the corresponding colours. $T = 240\,\mathrm{K}$, but the functional forms hold over the entire T range as witnessed by the parallel shift of the curves in **a**.

theory[26,27] predicts a change in the functional dependence for $d \ll l$ but cannot explain the observed f (Supplementary Information). At $T > 100$ K we find little variation in the measured ρ_{drag} for different contacts and devices with the same d. Drag also changes little after thermal cycling or annealing, although these procedures often change μ and occasionally shift the neutrality point. The high reproducibility and the well-defined d (compare with GaAlAs heterostructures) provide us with confidence in comparing the absolute value of ρ_{drag}. The inset in Fig. 2b and the Supplementary Information show that the measured drag exceeds the theoretical values (calculated according to ref. 27) by a factor of ≈ 3.

Anomalous drag in neutral graphene in zero and finite *B*

Now we focus on drag close to the dual neutrality point. In zero B and at high T, all our devices have exhibited positive drag at the dual neutrality point. Moreover, this positive drag often develops into a sharp peak with decreasing T. As an example, Fig. 3a shows the T dependence of $\rho_{drag}(n)$ for a device in which the peak was particularly pronounced. At 240 K, we observe the same double-humped behaviour as in Fig. 1d. At lower T, drag at the dual neutrality point first grows, which is opposite to the T dependence at finite n (Fig. 2). As a result, the curves become triple-humped below 150 K and the central peak dominates the low T curves, until drag eventually disappears under random-sign mesoscopic fluctuations[32,33].

The peak's strength varied from sample to sample so that, in some devices, it required $T < 70$ K to detect the central peak (Supplementary Information). The sample-dependent onset occurs because the T dependence at the dual neutrality point is non-monotonic (inset in Fig. 3a) whereas the general background varies as $\propto T^2$. Accordingly, central peaks with smaller strength require lower T to emerge. It is important to note that the central peak always appeared in the regime of e–h puddles. Their presence in each layer can be monitored by Hall measurements (Fig. 3b). At low T, the two extrema in $\rho_{xy}(n)$ indicate the crossover between a uniform Fermi liquid ($\rho_{xy} \propto 1/n$) and electron transport with a varying amount of e–h puddles ($\rho_{xy} \propto n$). We emphasize that the strongest peaks at the dual neutrality point were observed in devices with the widest e–h puddle regions, that is, with the largest δn. Thermal annealing could sometimes reduce δn, which resulted in weaker central peaks. No correlations with μ have been noticed. These observations suggest that the peak at the dual neutrality point in zero B is due to e–h puddles.

In GaAlAs heterostructures, Coulomb drag was found to exhibit its most interesting behaviour in the magnetic quantum limit where only the lowest Landau level remains occupied[4–11]. Accordingly, we have probed magneto-drag in our devices, focusing on this quantum limit that in graphene occurs at zero n. Away from the dual neutrality point, ρ_{drag} increases with increasing B and oscillates but these changes are relatively modest (Fig. 3c and Supplementary Information). The main qualitative change is found in the neutral state, in which case even relatively small B causes Coulomb drag to alter its sign. Figure 3c shows that this is an overwhelmingly strong effect such that $|\rho_{drag}|$ increases by a factor of >100 in $B < 1T$. In even larger $B > 10T$, the magneto-drag can reach $> 10\,k\Omega$. However, drag's behaviour in high B is complex (for example, the field opens energy gaps near the neutrality point (ref. 34), and individual graphene layers become increasingly insulating with increasing B at low T). Therefore, we limit our present report to moderate B, in which case drag exhibits the behaviour shown in Fig. 3b. It is highly reproducible from sample to sample and remains qualitatively the same for all our devices and only its magnitude changes with d (see Supplementary Information).

Possible origins of broken symmetry in neutral graphene

In the case of zero B, the peak at the dual neutrality point has already attracted two possible explanations[35,36]. One relies on third-order

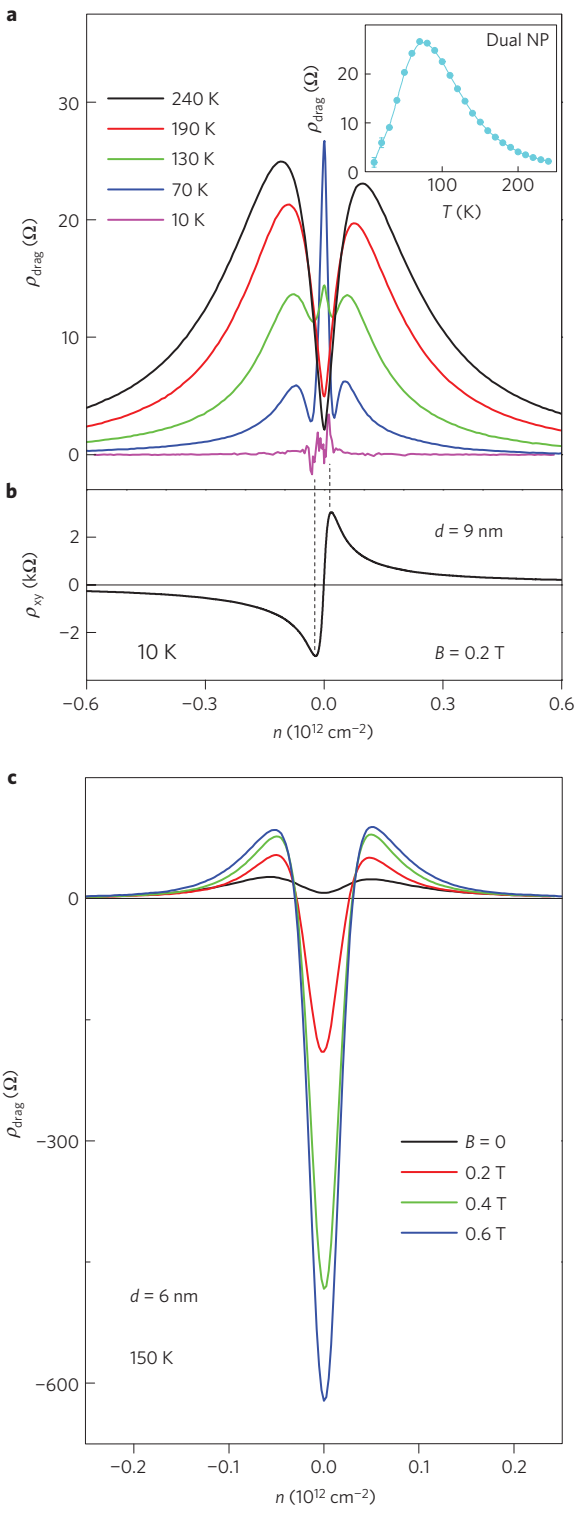

Figure 3 | Broken symmetry in neutral double-layer graphene. a, T dependence of $\rho_{drag}(n_T = -n_B \equiv n)$ in one of our devices in zero B; $d = 9$ nm. A sharp peak emerges at the dual neutrality point (NP) with decreasing T. Its T dependence is shown in the inset. The outside maxima in $\rho_{drag}(n)$ shift approximately linearly with T above 100 K. Their positions correspond to $E_F \approx 2T$, in agreement with ref. 26, which extends the drag theory into the Boltzmann regime. **b**, The regime of e–h puddles can be seen on $\rho_{xy}(n)$ curves as a transitional region indicated by the dashed lines. **c**, Typical changes in ρ_{drag} on applying B. Magneto-drag at zero n exhibits a non-monotonic T dependence such that it decreases with both increasing and decreasing T (see Supplementary Information).

interaction contributions that can be dominant at the neutrality point (ref. 35). This model does not capture the experimental fact that the central peak is related to e–h puddles. The second explanation attributes the peak to the interlayer energy transfer mediated by electron–electron interactions and explains many features in the observed behaviour[36]. We offer another explanation. As discussed in the Supplementary Information, if e–h puddles are due to an external electrostatic potential, their distribution in the two layers is correlated and, therefore, average drag at the dual neutrality point should be negative. We suggest that e–h puddles in our high-μ graphene are predominantly due to strain that results in a pseudo-electrostatic potential[37]. Under this assumption, e–h puddles are formed independently and remain independent if the two layers are far apart. However, for small d, Coulomb interaction leads to mutual polarization, and e puddles in one layer lie predominantly on top of h puddles in the other layer (Supplementary Information). This model explains the positive peak and accounts qualitatively for its T and n dependences. It is also consistent with the observation that the peak is large in devices with large δn.

As for strong negative magneto-drag at the neutrality point, no theory has been suggested so far. Nonetheless, the problem can be mapped onto the case of two half-filled Landau levels in GaAlAs heterostructures, which result in strong drag[4,6,9–11]. The associated interlayer many-body state is usually described in terms of condensation of excitons that consist of an electron in one layer (filling factor $\nu = 1/2$) bound to a vacancy-like state in the other $\nu = 1/2$ layer[4]. In high B, the parameter that controls the interaction strength is d/l_B, where l_B is the magnetic length. The observation of negative drag in GaAlAs heterostructures at the total filling factor $\nu_T = 1/2 + 1/2$ requires $d/l_B < 2$ (ref. 38) and values below 1 could not be achieved[4,6,9–11,38]. Owing to the Dirac-like spectrum, graphene's lowest Landau level ($N = 0$) is at zero energy so that, at the dual neutrality point, there are two half-filled Landau levels (ref. 39). As in the GaAlAs case, electrons at the $N = 0$ Landau level in one graphene layer can then pair with vacancy-like states at the $N = 0$ Landau level in the other layer. In GaAlAs devices, the observation of the excitonic drag requires modest $B \approx 1$–$2T$ but $T < 1$ K. It is surprising that strong interlayer correlations can apparently survive in graphene up to room temperature. To align this observation with intuition, we note first that the typical d/l_B in our experiment is ~ 0.1 (Fig. 3c), an order of magnitude smaller than in GaAlAs heterostructures. Second, our devices exhibit mobilities $\sim$100,000 cm^2 Vs^{-1}, practically independent of T. Therefore, the high field regime ($\mu B > 1$), in which cyclotron orbits are formed and d/l_B (rather than d/l) defines the interaction strength, is reached at $B > 0.1T$. Third, although the room-temperature quantum Hall effect in graphene is observable for $B > 20T$ (ref. 40), the build-up of the density of states at zero Landau level occurs in much lower B, as observed in capacitance measurements at room temperature (ref. 31). We believe that, under our experimental conditions, nascent $N = 0$ Landau levels assist the strong negative drag at the dual neutrality point but further work is necessary to understand this observation.

Outlook

Double-layer graphene heterostructures with ultrathin hBN spacers allow us to achieve unprecedentedly strong interactions between electrically isolated two-dimensional systems, especially in a magnetic field. In the Fermi liquid regime, the observed Coulomb drag is in agreement with theory, except for a factor of ≈ 3 in absolute value and an unexpected functional dependence on layer densities. In our opinion, the most interesting and previously unexplored regime is when both layers are neutral. In this case, strong sign-changing drag suggests broken e–h symmetries and new physics. In zero B, this can be explained by interaction-induced spatial correlations between e–h puddles. In a magnetic field, interlayer exciton-like correlations offer a tentative explanation for strong drag and invite one to search for high-T excitonic condensates. To investigate and understand double-layer graphene over a wide range of T and especially in quantizing B, much further work is needed, perhaps along the lines of enquiry being pursued for GaAlAs heterostructures during the past two decades.

Received 18 June 2012; accepted 6 September 2012; published online 14 October 2012; corrected online 19 October 2012

References

1. Solomon, P. M., Price, P. J., Frank, D. J. & La Tulipe, D. C. New phenomena in coupled transport between 2D and 3D electron-gas layers. *Phys. Rev. Lett.* **63,** 2508–2511 (1989).
2. Gramila, T. J., Eisenstein, J. P., MacDonald, A. H., Pfeiffer, L. N. & West, K. W. Mutual friction between parallel two-dimensional electron systems. *Phys. Rev. Lett.* **66,** 1216–1219 (1991).
3. Sivan, U., Solomon, P. M. & Shtrikman, H. Coupled electron-hole transport. *Phys. Rev. Lett.* **68,** 1196–1199 (1992).
4. Eisenstein, J. P. & MacDonald, A. H. Bose–Einstein condensation of excitons in bilayer electron systems. *Nature* **432,** 691–694 (2004).
5. Rojo, A. G. Electron-drag effects in coupled electron systems. *J. Phys.* **11,** 31–52 (1999).
6. Suen, Y. W., Engel, L. W., Santos, M. B., Shayegan, M. & Tsui, D. C. Observation of a $\nu = 1/2$ fractional quantum Hall state in a double-layer electron system. *Phys. Rev. Lett.* **68,** 1379–1382 (1992).
7. Eisenstein, J. P., Boebinger, G. S., Pfeiffer, L. N., West, K. W. & He, S. New fractional quantum Hall state in double-layer two-dimensional electron systems. *Phys. Rev. Lett.* **68,** 1383–1386 (1992).
8. Luhman, D. R. *et al.* Observation of a fractional quantum Hall state at $\nu = 1/4$ in a wide GaAs quantum well. *Phys. Rev. Lett.* **101,** 266804 (2008).
9. Kellogg, M., Eisenstein, J. P., Pfeiffer, L. N. & West, K. W. Vanishing Hall resistance at high magnetic field in a double-layer two-dimensional electron system. *Phys. Rev. Lett.* **93,** 036801 (2004).
10. Tutuc, E., Shayegan, M. & Huse, D. A. Counterflow measurements in strongly correlated GaAs hole bilayers: Evidence for electron–hole pairing. *Phys. Rev. Lett.* **93,** 036802 (2004).
11. Yoon, Y. *et al.* Interlayer tunneling in counterflow experiments on the excitonic condensate in quantum Hall bilayers. *Phys. Rev. Lett.* **104,** 116802 (2010).
12. Croxall, A. F. *et al.* Anomalous Coulomb drag in electron–hole bilayers. *Phys. Rev. Lett.* **101,** 246801 (2008).
13. Seamons, J. A., Morath, C. P., Reno, J. L. & Lilly, M. P. Coulomb drag in the exciton regime in electron–hole bilayers. *Phys. Rev. Lett.* **102,** 026804 (2009).
14. Lozovik, Y. E. & Yudson, V. I. Superconductivity at dielectric pairing of spatially separated quasiparticles. *Solid State Commun.* **19,** 391–393 (1976).
15. Min, H., Bistritzer, R., Su, J. J. & MacDonald, A. H. Room-temperature superfluidity in graphene bilayers. *Phys. Rev. B* **78,** 121401 (2008).
16. Kim, S. *et al.* Coulomb drag of massless fermions in graphene. *Phys. Rev. B* **83,** 161401 (2011).
17. Pillarisetty, R. *et al.* Coulomb drag near the metal–insulator transition in two dimensions. *Phys. Rev. B* **71,** 115307 (2005).
18. Ponomarenko, L. A. *et al.* Tunable metal–insulator transition in double-layer graphene heterostructures. *Nature Phys.* **7,** 958–961 (2011).
19. Britnell, L. *et al.* Field-effect tunneling transistor based on vertical graphene heterostructures. *Science* **335,** 947–950 (2012).
20. Lee, G. H. *et al.* Electron tunneling through atomically flat and ultrathin hexagonal boron nitride. *Appl. Phys. Lett.* **99,** 243114 (2011).
21. Britnell, L. *et al.* Electron tunneling through ultrathin boron nitride crystalline barriers. *Nano Lett.* **12,** 1707–1710 (2012).
22. Tse, W. K., Hu, B. Y. K. & Das Sarma, S. Theory of Coulomb drag in graphene. *Phys. Rev. B* **76,** 081401 (2007).
23. Katsnelson, M. I. Coulomb drag in graphene single layers separated by a thin spacer. *Phys. Rev. B* **84,** 041407 (2011).
24. Peres, N. M. R., Lopes dos Santos, J. M. B. & Castro Neto, A. H. Coulomb drag and high-resistivity behavior in double-layer graphene. *Europhys. Lett.* **95,** 18001 (2011).
25. Hwang, E. H., Sensarma, R. & Das Sarma, S. Coulomb drag in monolayer and bilayer graphene. *Phys. Rev. B* **84,** 245441 (2011).
26. Narozhny, B. N., Titov, M., Gornyi, I. V. & Ostrovsky, P. M. Coulomb drag in graphene: perturbation theory. *Phys. Rev. B* **85,** 201405 (2012).
27. Carrega, M., Tudorovskiy, T., Principi, A., Katsnelson, M.I. & Polini, M. Theory of Coulomb drag for massless Dirac fermions. *New J. Phys.* **14,** 063033 (2012).
28. Amorim, B. & Peres, N. M. R. On Coulomb drag in double layer systems. *J. Phys.* **24,** 335602 (2012).
29. Kharitonov, M. Y. & Efetov, K. B. Excitonic condensation in a double-layer graphene system. *Semicond. Sci. Technol.* **25,** 034004 (2010).

30. Mayorov, A. S. *et al.* Micrometer-scale ballistic transport in encapsulated graphene at room temperature. *Nano Lett.* **11,** 2396–2399 (2011).
31. Ponomarenko, L. A. *et al.* Density of states and zero Landau level probed through capacitance of graphene. *Phys. Rev. Lett.* **105,** 136801 (2010).
32. Tutuc, E. & Kim, S. Magnetotransport and Coulomb drag in graphene double layers. *Solid State Commun.* **15,** 1283–1288 (2012).
33. Price, A. S., Savchenko, A. K., Narozhny, B. N., Allison, G. & Ritchie, D. A. Giant fluctuations of Coulomb drag in a bilayer system. *Science* **316,** 99–102 (2007).
34. Young, A. F. *et al.* Spin and valley quantum Hall ferromagnetism in graphene. *Nature Phys.* **8,** 550–556 (2012).
35. Schütt, M. *et al.* Coulomb drag in graphene near the Dirac point. Preprint at http://arxiv.org/abs/1205.5018 (2012).
36. Song, J. C. W. & Levitov, L. S. Energy-driven drag at charge neutrality in graphene. Preprint at http://arxiv.org/abs/1205.5257 (2012).
37. Gibertini, M., Tomadin, A., Guinea, F., Katsnelson, M. I. & Polini, M. Electron-hole puddles in the absence of charged impurities. *Phys. Rev. B* **85,** 201405 (2012).
38. Kellogg, M., Eisenstein, J. P., Pfeiffer, L. N. & West, K. W. Bilayer quantum Hall systems at $\nu_T = 1$: Coulomb drag and the transition from weak to strong interlayer coupling. *Phys. Rev. Lett.* **90,** 246801 (2003).
39. Castro Neto, A. H., Guinea, F., Peres, N. M. R., Novoselov, K. S. & Geim, A. K. The electronic properties of graphene. *Rev. Mod. Phys.* **81,** 109–162 (2009).
40. Novoselov, K. S. *et al.* Room temperature quantum Hall effect in graphene. *Science* **315,** 1379 (2007).

Acknowledgements

We thank L. Levitov, M. Titov and A. Castro Neto for helpful discussions. This work was supported by the Royal Society, the Körber Foundation, Engineering and Physical Sciences Research Council (UK), the Office of Naval Research and the Air Force Office of Scientific Research.

Author contributions

L.A.P., R.V.G. and A.K.G. devised the project. K.W. and T.Ta. provided hBN crystals. R.V.G. designed and fabricated the heterostructures. L.A.P. carried out measurements and analysed the results. M.I.K., T.Tu. and A.H.M. provided theoretical support. A.K.G. wrote the paper. M.I.K. and T.Tu drafted the theory part of the Supplementary Information. K.S.N., I.V.G. and S.V.M. helped with experiments and/or writing the paper. All authors contributed to discussions.

Additional information

Supplementary information is available in the online version of the paper. Reprints and permissions information is available online at www.nature.com/reprints. Correspondence and requests for materials should be addressed to L.A.P.

Competing financial interests

The authors declare no competing financial interests.

ERRATUM

Strong Coulomb drag and broken symmetry in double-layer graphene

R. V. Gorbachev, A. K. Geim, M. I. Katsnelson, K. S. Novoselov, T. Tudorovskiy, I. V. Grigorieva, A. H. MacDonald, S. V. Morozov, K. Watanabe, T. Taniguchi and L. A. Ponomarenko

Nature Physics http://dx.doi.org/10.1038/nphys2441 (2012); published online 14 October 2012; corrected online 19 October 2012.

In the version of this Article originally published online, the unit on the *y* axis of Fig. 3c was incorrect, it should have read "ρ_{drag} (Ω)". This error has been corrected in all versions of the Article.